validate (3), We evaluated Dice's coefficient to verify shape similarity between pCT and rCT delineations (figure 2F). Values near 1 indicate shape preservation except for kidneys, as these intersect the ROI superior boundary where non-rigid transformations were applied.

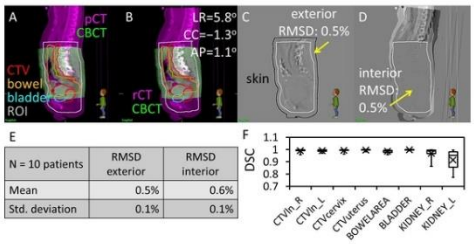

N = 10 patients	RMSD exterior	RMSD interior
Mean	0.5%	0.6%
Std. deviation	0.1%	0.1%

Figure 2. (A) Overlay of planning CT (pCT) with CBCT and (B) simulated rCT with CBCT. (C) Grey value differences between pCT and rCT, show minimal RMSD in the region exterior to the ROI. (D) Registration of rCT back to the pCT shows minimal RMSD within the ROI. (E) Summary RMSD statistics for 10 patients. (F) Dice similarity coefficient (DSC) close to 1 verifies shape similarity between pCT and rCT delineations.

Conclusion

Simulation of a repeat CT scan based on RBFs successfully corrects pelvic rotations, while maintaining minimal skin displacement and preserving tumor and OAR shapes. To manage *systematic* rotations, the simulated rCT should be based on the average registration of *N* CBCTs. The proposed method is a highly efficient alternative for repeat CT scanning to adapt pelvic treatment plans for systematic rotations.

Reference:

1. M. Fornefett, K. Rohr and H.S. Stiehl. Image and Vision Computing 19, 87-96 (2001).

EP-2054 Potential role of dual-energy CT imaging modality in the neoadjuvant radiotherapy: a phantom study

P. Gallo[1], A. D'Alesssio[2], F. Padelli[3], M.L. Fumagalli[1], E. D'ippolito[2], T. Giandini[2], C. Tenconi[2], C. Cavatorta[2], M.G. Bruzzone[3], E. Pignoli[2], E. De Martin[1]

[1]Fondazione IRCCS Istituto Neurologico Carlo Besta, Health Department, Milan, Italy ; [2]Fondazione IRCCS Istituto Nazionale dei Tumori di Milano, Medical Physics Unit, milan, Italy ; [3]Fondazione IRCCS Istituto Neurologico Carlo Besta, Neuroradiology Department, Milan, Italy

Purpose or Objective

Purpose/Objective:

Dual-energy CT (DECT) is a more and more widespread technique based on the merging of two CT scans acquired at different tube potentials (80 and 140 kVp) to improve differentiation of materials and patient tissues. Images obtained through virtual monoenergetic reconstruction (MONO) can improve image quality compared with conventional single-energy CT scanning (SECT). The purpose of this study is to investigate potential applications of MONO reconstructions to improve soft-tissue contrast with no need of contrast medium injection, and consequent repercussions on target volume identification and delineation.

Material and Methods

The CIRS® Electron Density Phantom containing different tissue-equivalent inserts was imaged using two CT scanners: Siemens Somatom Confidence (sequential scanning at two tube voltages) and General Electric (GE) Revolution GSI (rapid switching of tube voltage). SECT and DECT acquisitions were performed maintaining a similar dose level and MONO images were than reconstructed at various energies levels (40, 50, 70, 100, 120, 140, 190 keV). In the first step of our analysis, both SECT and DECT images were reconstructed through a Filter Back Projection (FBP) algorithm. CT numbers and their standard deviations were measured within the CIRS® inserts to evaluate different contrasts (breast-adipose, muscle-adipose, liver-adipose) of MONO reconstructions with respect to SECT images.

Results

In general, a soft-tissue signal enhancement was observed with the decrease of MONO images reconstruction energy. The greatest signal enhancement is observed at 40 and 50 keV compared to SECT for adipose and breast inserts for both scanners (Figure 1). Moreover, at 40 keV breast-adipose CT number contrast results in +48% and +45% for GE and Siemens respectively when compared to SECT data.At 50 keV this contrast enhancement is still observable (+19% and +14% for GE and Siemens respectively). As expected, higher energy MONO reconstructions show less contrast with respect to SECT data (Table1).

Conclusion

Conclusion:

Low energy (40-50 keV) DECT MONO reconstructions increase soft-tissue contrast, potentially allowing a better radiotherapy target volume identification and delineation, in particular when breast and pelvic anatomy are involved. The increased image noise associated with lower MONO energies could be at least partially compensated by using iterative reconstruction algorithms. Our results suggest that a great advantage might be achievable for example in the neoadjuvant radiotherapy of breast cancer, especially in the partial breast irradiation with ablative intent.

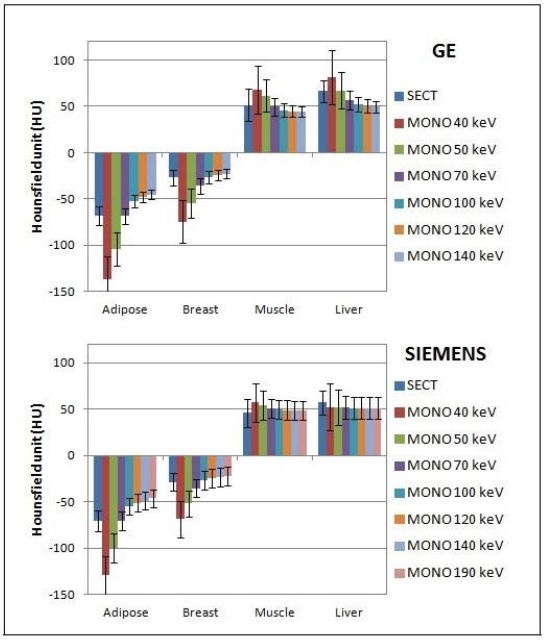

Figure 1: CT numbers measured on SECT and DECT images of CIRS® Electron Density Phantom

Table1: Contrast variation between Dual Energy CT and Single Energy CT acquisitions.

CT Scanner	Tissue contrast	Contrast variations (%) between DECT and SECT acquisition.						
		40 keV	50 keV	70 keV	100 keV	120 keV	140 keV	190 keV
SIEMENS	*BREAST-ADIPOSE*	45%	14%	-16%	-32%	-36%	-39%	-41%
	MUSCLE-ADIPOSE	60%	32%	4%	-10%	-14%	-16%	-18%
	LIVER-ADIPOSE	42%	19%	-4%	-17%	-20%	-22%	-24%
GE	*BREAST-ADIPOSE*	48%	19%	-22%	-39%	-43%	-46%	//
	MUSCLE-ADIPOSE	70%	38%	-2%	-18%	-23%	-26%	//
	LIVER-ADIPOSE	61%	27%	-7%	-23%	-27%	-30%	//

EP-2055 Impact of patient-specific MRI distortion correction for stereotactic cranial target definition

T. Gevaert[1], B. Engels[1], C. El Aisati[1], M. De Ridder[1]

[1]Universitair Ziekenhuis Brussel, Radiotherapy, Brussels, Belgium

Purpose or Objective
The accuracy of a stereotactic treatment is primarily limited by the least accurate process in the whole chain of events from patient scanning to patient treatment. The total error is accumulated through the processes of a) target localization and planning using medical imaging (computed tomography (CT) and magnetic resonance imaging (MRI), image fusion, dose planning, and b) dose delivery using image guidance patient positioning, immobilization devices and a radiation dose delivery system.
QA is often performed on the dose delivery and planning section rather than the localization. This targeting is primarily limited by the accuracy of the CT and MRI images. In theory CT scans are precise. In contrast, MRI datasets are subjected to distortions, due to nonlinearity of gradient fields, and may cause incorrect target definition.
This study aimed to analyze the impact of a patient-specific algorithm, Crainial distortion Elements (Brainlab, München, Gernmany, rather than a manufacture-specific, to correct spatial distortion in cranial magnetic resonance images.
Material and Methods
Twelve trigeminal patients treated with a single dose of 90 Gy with a 4mm collimator were studied retrospectively. A radiosurgery target (gross target volume ((GTV)) was defined on a 1.0mm T1 MPRAGE and T2 MRI corrected for distortion with a machine-specific algorithm.
For this study, the manufacture-specific corrected MRI was further corrected using a patient-specific distortion correction algorithm that references the treatment planning CT. The GTV were then mapped onto this newly created patient specific corrected MRI dataset. The original defined target and the corrected deformed object were mutually compared by means of several quantitative measures such as Dice, Jaccard, and Hausdorff indices. The average distance between the two centers of the two GTV was also calculated.
Results
On average, a good agreement was found between both GTV resulting in a Dice index of 0.76 (SD 0.23) ranging between 0.13 and 0.92. The Jaccard index, which is an intersection over Union was similar ($p > 0.1$) to the Dice with an average of 0.66 (SD 0.23) ranging between 0.09 and 0.86. The greatest of all the distances from a point in GTV to the closest point in the other GTV, called the Hausdorff distance, was 0.73 on average (range 0.50 - 1.80), reflecting good similarity between both GTVs. Average distance between both GTV was 0.43 mm (SD 0.26mm), with a minimum of 0.20 mm and a maximum of 1.10 mm. One out of the 12 patients met criteria of "geometric miss", which was not correlated with clinical outcome.
Conclusion
Although MRI distortion is often corrected manufacture specific, distortion may persist due to patient specific conditions. Our study showed that the cranial distortion Elements correct all images even when manufacture-specific corrections fail. In order to avoid any geometrical miss, a patient specific distortion correction must be applied for all cranial indication.

EP-2056 Feasibility of realistic Digitally Reconstructed Radiograph (DRR) rendering through shallow learning

J. Dhont[1,2], J. Vandemeulebroucke[1], I. Mollaert[3], D. Verellen[2,3]
[1]Vrije Universiteit Brussel, Department of Electronics and Informatics ETRO, Brussels, Belgium ; [2]Vrije Universiteit Brussel, Faculty of Medicine and Pharmaceutical Sciences, Brussels, Belgium ; [3]GZA Ziekenhuizen campus Sint-Augustinus- Iridium kankernetwerk, Department of Medical Physics, Antwerp, Belgium

Purpose or Objective
Accurate DRRs with realistic soft-tissue contrast could aid markerless tumor tracking. Purpose of this study is to investigate the feasibility of accurate DRR rendering using a shallow neural network (NN) that models the CT-to-Xray intensity, including non-linear effects such as beam-hardening, omitting multiple phantom measurements and Xray source modeling.
Material and Methods
To overcome the black box character of deep-learning (DL), this study was divided into several controlled steps. Initially, real-patient data was omitted to avoid object deformations, and input and output data was rendered using a static CIRS thorax phantom. One planning CT image (512*512*328, 1 mm slice thickness, 1.1x1.1 mm^2 in-plane res., Toshiba) and one full-fan CBCT image (TrueBeam STx, Varian) were acquired, of which only the anterior-posterior (AP) projection image (1024*768 pxs, 0.39 x 0.39 mm^2, res.) was used.
To render input for the NN, a ray-tracing algorithm was developed in Matlab, see Figure 1. Taking into account the CBCT acquisition geometry, the nearest CT voxel was sampled every 1 mm on a straight line from the Xray source to each pixel in the AP projection image, resulting in 1024*768 rays. Per ray, most surrounding was discarded, keeping 500 samples per ray centered around the phantom as input to the model.
Secondly, to determine the model topology and optimize the hyper-parameters while keeping other degrees of freedom to a minimum, the line integral over each ray was taken as the output target value for each ray, creating a raw DRR value. In total 1024*768 input-output couples were generated, of which 24% were discarded to avoid imbalance. Of the remainder, 98% was used to determine model topology, for hyper-parameter optimization and for training, while 2% was used for validation, sampled randomly.
A shallow feed-forward regression network, see Figure 1, was created using TensorFlow, consisting of an input layer of 500 nodes, one single-node fully-connected hidden layer with rectified linear activation (ReLu) function, and a single-node output layer. Stochastic gradient descent was used to optimize the network weights and the loss function was minimized based on the mean squared error (MSE). The network accuracy was evaluated using student's t-test to determine the statistical significance of the difference between the predicted and ground-truth output values in the validation data-set.

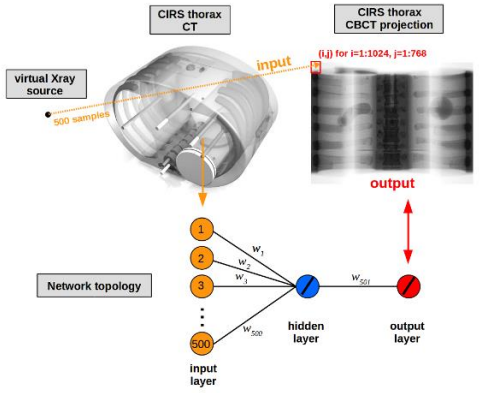

Figure 1: A ray-tracing algorithm was used to sample the CT image and generate 500 input samples per ray, for every pixel in the corresponding projection image, whose values will be used as targets in the illustrated network topology.

Results
Student's t-test showed no significant difference between the predicted and ground-truth output values ($p < 0.001$), with maximum intensity differences of 0.1%.